European Journal of Pharmaceutics and Biopharmaceutics 74 (2010) 451–460

Contents lists available at ScienceDirect

European Journal of Pharmaceutics and Biopharmaceutics

journal homepage: www.elsevier.com/locate/ejpb

Research paper

Detection of early colorectal cancer imaged with peanut agglutinin-immobilized fluorescent nanospheres having surface poly(*N*-vinylacetamide) chains

Shinji Sakuma [a,*], Takanori Yano [a], Yoshie Masaoka [a], Makoto Kataoka [a], Ken-ichiro Hiwatari [b], Hiroyuki Tachikawa [b], Yoshikazu Shoji [b], Ryoji Kimura [b], Huaiyu Ma [c], Zhijian Yang [c], Li Tang [c], Robert M. Hoffman [c,d], Shinji Yamashita [a]

[a] *Faculty of Pharmaceutical Sciences, Setsunan University, Osaka, Japan*
[b] *Advanced Materials R&D Laboratory, ADEKA Co., Tokyo, Japan*
[c] *AntiCancer Inc., CA, USA*
[d] *Department of Surgery, University of California at San Diego, CA, USA*

ARTICLE INFO

Article history:
Received 30 September 2009
Accepted in revised form 5 January 2010
Available online 10 January 2010

Keywords:
Imaging
Endoscopic imaging agent
Colorectal cancer
Peanut agglutinin
Poly(*N*-vinylacetamide)

ABSTRACT

Peanut agglutinin (PNA)-immobilized fluorescent nanospheres were designed as a novel imaging agent for colonoscopy. PNA is a targeting moiety that binds to β-D-galactosyl-(1–3)-*N*-acetyl-D-galactosamine, which is the terminal sugar of the Thomsen-Friedenreich antigen that is specifically expressed on the mucosal side of colorectal cancer cells. The in vivo performance of the imaging agent was evaluated using a human colorectal cancer orthotopic animal model. Human colorectal adenocarcinoma cell lines, HT-29, HCT-116, and LS174T, were implanted on the cecal serosa of immune-deficient mice. A loop of the tumor-bearing cecum was made, and the luminal side was treated with the imaging agent. Strong fluorescence was observed at several sites of the cecal mucosa, irrespective of cancer cell type. Microscopic histological evaluation of the cecal mucosa revealed that bright areas with fluorescence derived from the imaging agent and dark areas without the fluorescence well denoted the presence and absence, respectively, of the invasion of implanted cancer cells on the mucosal side. This good correlation showed that PNA-immobilized fluorescent nanospheres recognized millimeter-sized tumors on the cecal mucosa with high affinity and specificity.

1. Introduction

Colorectal cancer, which is one of the major causes of mortality and morbidity in developed countries, is primarily treated by surgical resection [1,2]. Early detection is critical for successful treatment [2–4]. Colonoscopy has been effectively used for screening colorectal cancer with its ability to provide a definitive diagnosis. The cancer that remains in the mucous membrane or only minimally invades the submucosal tissues without vessel invasion is often treated by resection using endoscopy. This minimally invasive operation, known as endoscopic mucosal resection (EMR), can serve as an alternative to surgical resection in the early stage of the cancer [5–7]. While the colonoscopy procedure is critically important, standard white-light colonoscopy has a major limitation: it can only detect tumor tissues that are larger than ca. 1 cm in size. Tumors of this size have a relatively high probability of metastasis [4,8]. Magnifying endoscopy has contributed to the detection of small-sized colorectal cancer; however, accurate differentiation of neoplastic mucosal changes in real-time remains a significant challenge [9,10]. Thus, there is a great need for developing an endoscopic imaging agent that can provide early detection of small-sized colorectal cancer [11], as well as novel imaging strategies for endoscopy such as narrow band imaging and autofluorescence imaging [9,10,12–14].

Colorectal cancer first develops in the mucous membrane of the large intestine. We previously designed an imaging agent that can recognize tumor-derived changes on the mucosal side of epithelial cells in the large intestine with high affinity and specificity [15]. The agent comprises submicron-sized fluorescent polystyrene nanospheres with two functional groups – peanut (*Arachis hypogaea*) agglutinin (PNA) and poly(*N*-vinylacetamide) (PNVA) – on their surfaces. The Thomsen-Friedenreich (TF) antigen is expressed specifically on the mucosal side of colorectal cancer cells [16–19]. In normal cells, the terminal sugar of the TF antigen is masked by oligosaccharide side chain extension or by sialylation. PNA was immobilized on the nanosphere surface as a targeting moiety that binds to the TF antigen with high affinity and specificity through

* Corresponding author. Faculty of Pharmaceutical Sciences, Setsunan University, 45-1 Nagaotoge-cho, Hirakata, Osaka 573-0101, Japan. Tel.: +81 72 866 3124; fax: +81 72 866 3126.
E-mail address: sakuma@pharm.setsunan.ac.jp (S. Sakuma).

0939-6411/$ - see front matter © 2010 Elsevier B.V. All rights reserved.
doi:10.1016/j.ejpb.2010.01.001

the recognition of the terminal sugar, β-D-galactosyl-(1–3)-*N*-acetyl-D-galactosamine (Gal-β(1–3)GalNAc) [20,21]. However, the tumor-derived change in the large intestinal mucosa is very small throughout the entire large intestine. To detect such a small change accurately, the imaging agent should have a strong affinity for targets (i.e., cancer tissues) with minimal nonspecific interactions with nontargets (i.e., normal tissues). PNVA, which is a nonionic polymer with strong hydrophilicity, was also immobilized on the nanosphere surface to enhance the specificity of PNA by reducing the nonspecific interactions between the imaging agent and normal tissues [22,23]. Coumarin 6, which is a commercial product with high fluorescence quantum efficiency, was used as the fluorescent dye that provides an endoscopically detectable fluorescence intensity. It was encapsulated into the polystyrene cores of the nanospheres through their strong hydrophobic interactions [24]. It is anticipated that intracolonic (enema) administration of PNA-immobilized fluorescent nanospheres having surface PNVA chains (i.e., imaging agent) leads to their specific accumulation on the surface of tumor tissues in the large intestine with resulting fluorescence. Real-time and accurate diagnosis of small-sized early colorectal cancer can be then achieved through observations of a clear fluorescence contrast between the normal and tumor tissues using the standard fluorescence endoscopy with or without magnification.

In a series of research, the hemagglutination test, which is often used for the assay of lectin activities, was first performed to optimize the chemical structure of the imaging agent [15]. PNA-immobilized fluorescent nanospheres with different chemical structures were prepared, and the activity of PNA immobilized on the nanosphere surface was evaluated. By adjusting the molecular weight of PNVA, we consequently obtained PNA-immobilized fluorescent nanospheres with surface PNVA chains whose affinity and specificity for Gal-β(1–3)GalNAc detection were equivalent and superior, respectively, to those of intact PNA. Interactions between the imaging agent and various types of cultured human cells were next evaluated [24]. The in vitro cell studies demonstrated that the imaging agent bound to TF antigen-expressing cancer cells with high affinity and specificity. This was likely due to the recognition of Gal-β(1–3)GalNAc by the imaging agent. Preliminary in vivo studies were also carried out using nude mice bearing ascending colon tumors derived from the HT-29 human colorectal adenocarcinoma cell line. Imaging agent-derived fluorescence was observed at several sites of the colonic mucosa in tumor tissue-implanted mice after the luminal side of the colon was treated with the imaging agent. Specific accumulation of the imaging agent was not observed in nude mice without colon tumors. This macroscopic observation suggested that the imaging agent specifically bound to HT-29-derived tumors on the mucosal surface of the colon.

A goal of our research is to develop an endoscopic imaging agent that enables real-time and accurate diagnosis of small-sized colorectal cancer. Successive in vivo studies were performed with the aim of describing the imaging of early colorectal cancer with PNA-immobilized fluorescent nanospheres having surface PNVA chains whose chemical structure was optimized in our previous study [15].

2. Materials and methods

2.1. Materials

NVA monomers were a gift from Showa Denko Co. (Tokyo, Japan). Coumarin 6 and PNA were obtained from Sigma–Aldrich (St. Louis, MO, USA). Dextran sulfate sodium (DSS; Mw: 25,000) was purchased from Tokyo Kasai Industry Co., Ltd. (Tokyo, Japan). All other chemicals were commercial products of reagent grade.

The human colorectal adenocarcinoma cell lines, HT-29, HCT-116, and LS174T, were purchased from Dainippon-Sumitomo Pharma Biomedical Co., Ltd. (Osaka, Japan). The following media were obtained from Sigma–Aldrich: RPMI-1640 Medium; McCoy's 5A Medium, Modified (with sodium bicarbonate, without L-glutamine); Minimum Essential Medium Eagle; Dulbecco's Modified Eagle's Medium; Dulbecco's Phosphate Buffered Saline (PBS with calcium chloride and magnesium chloride); Dulbecco's Phosphate Buffered Saline, Modified (PBS without the divalent metal ions). Fetal bovine serum (FBS), heat-inactivated FBS, penicillin (10,000 U/mL), streptomycin (10 mg/mL), L-glutamine (200 mM), nonessential amino acids (10 mM), and trypsin–EDTA (0.25% trypsin and 1 mM EDTA) were purchased from GIBCO Laboratories (Lenexa, KS, USA). Preserved rabbit blood and neuraminidase (sialidase, 1 unit/mL, extracted from *Arthrobacter ureafaciens*) were obtained from Nippon Bio-Test Laboratories Inc. (Tokyo, Japan) and Roche Diagnostics (Indianapolis, IN, USA), respectively.

The $pLNC_{X2}$ vector, which contains the neomycin resistance gene for antibiotic selection in eukaryotic cells, the red fluorescent protein (RFP, DsRed2), and RePT67 (an NIH 3T3-derived packaging cell line expressing the 10 Al viral envelope) were purchased from Clontech (Mountain View, CA, USA). G418 and cloning cylinders were obtained from Roche Molecular Biochemicals (Indianapolis, IN, USA) and Bel-Art Products (Pequannock, NJ, USA), respectively.

2.2. Preparation and characterization of the imaging agent

Preparation procedures for the imaging agent have been described previously [24]. Briefly, PNVA and poly(*tert*-butyl methacrylate) (PBMA) were prepared by the free radical polymerization of NVA and butyl methacrylate (BMA) monomers, respectively, in the presence of 2-mercaptoethanol. The resulting hydroxyl group-terminated PNVA and PBMA were reacted with *p*-chloromethyl styrene in the presence of tetrabutylphosphonium bromide in an alkaline solution. Vinylbenzyl group-terminated PMAA was obtained by hydrolyzing vinylbenzyl group-terminated PBMA in an acidic solution with hydroquinone. Fluorescent nanospheres having surface PNVA and PMAA chains (a precursor of the imaging agent) were prepared by dispersion copolymerization between vinylbenzyl group-terminated PNVA, vinylbenzyl group-terminated PMAA, and styrene at a weight ratio of 1:1:2 in an ethanol/water mixture containing 2,2′-azobisisobutyronitrile and coumarin 6 (0.1% of the total monomers). After the unreacted substances and unencapsulated coumarin 6 were removed by centrifugation, PNA was bound to the fluorescent nanospheres through the coupling of amino groups of PNA with carboxyl groups of PMAA activated by pre-incubation with 1-ethyl-3-(3-dimethylaminopropyl)carbodiimide. The resulting PNA-immobilized fluorescent nanospheres having surface PNVA chains (i.e., imaging agent) were purified and then dispersed in purified water at a concentration of 20 mg/mL.

Routine characterization of the imaging agent and its precursor was performed as described previously [15,22–26]. Briefly, weight- and number-average molecular weights of the surface PNVA and PMAA chains were determined by gel permeation chromatography. The nanosphere size was measured by dynamic light-scattering spectrophotometry. The zeta potential of the nanospheres was measured by electrophoretic light-scattering spectrophotometry in PBS (without divalent metal ions). The ratio of the number of NVA units to that of MAA units on the nanosphere surface was evaluated by electron spectroscopy for chemical analysis. The amount of coumarin 6 encapsulated into the nanosphere core was measured by spectrophotometry. The amount of PNA immobilized on the nanosphere surface was measured by the ninhydrin method. The affinity and specificity of immobilized PNA for recognition of Gal-β(1–3)GalNAc were evaluated using the hemagglutination test.

2.3. Human colorectal cancer orthotopic animal model

2.3.1. Orthotopic implantation nude mouse model

A red fluorescent protein (RFP)-expressing human colorectal cancer orthotopic animal model was constructed as follows [27–29].

The RFP gene (DsRed2) was inserted in the $pLNC_{X2}$ vector at the *Egl*II and *Not*I sites. PT67 cells were cultured in Dulbecco's Modified Eagle's Medium supplemented with 10% (v/v) heat-inactivated FBS. For vector production, packaging cells (PT67), at 70% confluence, were incubated with G418 and saturating amounts of $pLNC_{X2}$-DsRed2 plasmid for 18 h. Fresh medium was replenished at this time. The cells were examined by fluorescence microscopy 48 h after transfection. For selection, the cells were cultured in the presence of 500–2000 μg/mL of G418 for 7 days.

For RFP gene transduction, 25% confluent HCT-116 cells were incubated with a 1:1 precipitated mixture of retroviral supernatants of PT67 cells and RPMI-1640 Medium containing 10% (v/v) FBS for 72 h. Fresh medium was replenished at this time. Cells were harvested by trypsin–EDTA 72 h after transduction and subcultured at a ratio of 1:15 into a selective medium that contained 200 μg/mL of G418. The level of G418 was increased to 400 μg/mL in a stepwise manner. Clones stably expressing RFP were isolated with cloning cylinders by trypsin–EDTA and were then amplified, and transferred by conventional culture methods in the absence of a selective agent.

All animal studies were conducted in accordance with the principles and procedures outlined in the National Institute of Health Guide for the Care and Use of Animals under Assurance Number A3873-1. All surgical procedures and animal manipulations were conducted under HEPA-filtered laminar-flow hoods. Nude mice, 4-week-old outbred nu/nu female mice, were used for tumor tissue implantation. A tumor stock of HCT-116-RFP was established by subcutaneously injecting HCT-116-RFP cells (1×10^6 cells/mL) into the flank of nude mice. The tumor was maintained in the nude mice subcutaneously as tumor stock prior to being used. On the day of implantation, the tumor was harvested from the subcutaneous site and placed in RPMI-1640 Medium. Strong RFP expression of the HCT-116-RFP tumor tissues was confirmed by fluorescence imaging. Necrotic tissues were removed, and viable tissues were cut into 1 mm^3 pieces. The nude mice were transplanted by surgical orthotopic implantation using tumor tissue fragments harvested from the stock tumors. The animals were anesthetized with a mixture of ketamine, acepromazine, and xylazine, and the surgical area was sterilized using iodine solution and alcohol. An incision approximately 1.5 cm long was made along the left lateral abdomen of the nude mouse using a pair of sterile scissors. After the abdomen was opened, the ascending colon was exposed. The serosa of the transplantation site was stripped. Two fragments of the HCT-116-RFP tumor tissues (1 mm^3) were sutured adjacent to each other onto the ascending colon with a sterile 8-0 surgical suture (nylon) to generate only one primary tumor. The abdomen was closed using sterile 6-0 surgical sutures (silk). Nude mice bearing ascending colon tumors obtained were maintained for a predetermined period until implanted tumor tissues invaded the mucosal side of epithelial cells.

2.3.2. Orthotopic implantation SCID mouse model

Orthotopic implantation of human colorectal cancer cells was conducted using a minor modification of the procedures reported by Zamai et al. [30].

Human colorectal cancer cells were seeded at a density of 2×10^4 cells/mL (HT-29 and HCT-116) or 6×10^4 cells/mL (LS174T) in a flask of adequate volume (25–75 mL). Minimum Essential Medium Eagle supplemented with 10% (v/v) FBS, 50 U/mL penicillin, 50 μg/mL streptomycin, and 0.1 mM nonessential amino acids was used as a medium for LS174T. McCoy's 5A Medium, Modified supplemented with 10% (v/v) FBS, 50 U/mL penicillin, 50 μg/mL streptomycin, and 1.5 mM L-glutamine was used as a medium for the other cancer cells. The cells were grown as a monolayer in the media and were maintained at 37 °C in a humidified atmosphere of 95% O_2/5% CO_2. Cells were then routinely passaged when they became 100% confluent, and the low passage cell lines (passage: $\leqslant$10 times) were used.

Animal experiments were approved by the Ethical Review Committee of Setsunan University. All surgical procedures and animal manipulations were conducted under HEPA-filtered laminar-flow hoods. Severe combined immunodeficiency (SCID) mice, 6-week-old C.B-17/Icr SCID/SCID female mice, were used for cancer cell implantation. Cancer cells were washed with 20 mL of PBS (without divalent metal ions) after the removal of the culture media. PBS was removed, and the cells were treated at 37 °C for 3 min with 2 mL of the aqueous solution containing trypsin–EDTA. A corresponding culture medium (10 mL) was added to remove the cells from the flask. The collected cells were centrifuged at 180 g for 10 min, and the precipitated cells were suspended in PBS (with divalent metal ions) at a concentration of 4×10^7 cells/mL. The animals were anesthetized with ether, and the surgical area was sterilized using ethanol (70%, v/v). An incision approximately 1.5 cm long was made along the left lateral abdomen of the SCID mouse using a pair of sterile scissors. After the abdomen was opened, the cecum was exposed. The cell suspension (1×10^6 cells/0.025 mL) was injected into cecal serosa of the SCID mouse, and the abdomen was then closed. SCID mice bearing cecal tumors obtained were maintained for a predetermined period until implanted cancer cells invaded the mucosal side of epithelial cells.

2.4. In vivo biorecognition of the imaging agent for orthotopic human colorectal tumors

2.4.1. Orthotopic implantation nude mouse model

Nude mice bearing ascending colon tumors were fasted for 24 h with free access to water before experiments. Under ether anesthesia, the abdomen was opened, and the ascending colon, in which HCT-116-RFP tumor tissues had been implanted, was observed. An approximately 3-cm loop of the tumor-bearing ascending colon was prepared in the abdomen by ligating both ends of the colon after washing the luminal side with saline. The imaging agent was dispersed in PBS (with divalent metal ions) at a concentration of 4 or 20 mg/mL. One milliliter of the dispersion was injected into the loop. At 30 min after injection, the loop was removed and its luminal side was washed with $\geqslant$1 mL of PBS (with divalent metal ions). The incubation time was reduced to 10 min when the concentrated dispersion (20 mg/mL) was used. The colon was cut longitudinally and a fluorescence microphotograph of the mucosal surface was taken using a fluorescence microscope (IX71-22FL/PH; Olympus Co., Ltd., Tokyo, Japan; excitation: 470–495 nm; emission: 510–550 nm; exposure: 1/15–1/60 of a second). For the evaluation of the autofluorescence of tumor tissues in the colon, an equivalent volume of PBS (with divalent metal ions) was substituted for the imaging agent dispersion.

2.4.2. Orthotopic implantation SCID mouse model

As described above for nude mice, an approximately 3-cm loop of the tumor-bearing cecum was prepared in the abdomen of SCID mice by ligating both junctions of the cecum to the ileum and ascending colon after washing the luminal side of the cecum with saline. The dispersion of the imaging agent (20 mg/mL, 1.0 mL) was injected into the loop. At 1, 10, or 30 min after injection, the loop was removed and its luminal side was washed with $\geqslant$1 mL of PBS (with divalent metal ions). The cecum was cut longitudinally, and the mucosal surface was observed with the fluorescence

microscope. As a control, normal SCID mice that did not undergo cancer cell implantation were tested in the same manner as that described above. The autofluorescence of normal and tumor tissues in the cecum was evaluated as described in Section 2.4.1.

After imaging, the cecum was cut into small pieces of approximately 2–3 mm in length. The mucosal surface of each piece was observed with the fluorescence microscope, and the pieces were classified into bright ones with fluorescence derived from the imaging agent and dark ones without the fluorescence. Each piece was fixed with formaldehyde aqueous solution (10%, v/v) and then sectioned at 3 μm thickness at 200–300-μm intervals. Mucosal invasion was evaluated histologically using three slices that corresponded to positions at which the piece was divided equally in four parts.

2.5. Specificity of the imaging agent for DSS-induced ulcerative colitis

SCID mice, 6-week-old C.B-17/Icr SCID/SCID female mice, were used. Acute colitis was induced by 9 days of administration of DSS aqueous solution (5%, w/v) in the drinking water [31]. Animals with bloody diarrhea were sacrificed for the experiment. An approximately 3-cm loop of the descending colon was prepared by ligating both ends of the colon as described above. The specificity of the imaging agent for DSS-induced ulcerative colitis was then assessed in the same manner as that described in Section 2.4.2.

3. Results and discussion

3.1. Characterization of the fluorescent nanospheres having surface PNVA and PMAA chains and PNA-immobilized ones

The imaging agent was synthesized according to Scheme 1. Table 1 summarizes the characterization of the fluorescent nanospheres having surface PNVA and PMAA chains (a precursor of the imaging agent) and the PNA-immobilized ones (the imaging agent). PNVA with an Mw (weight-average molecular weight)/Mn (number-average molecular weight) of 9500/4000 and PMAA with an Mw/Mn of 10,000/5600 were used. MAC, i.e., the minimum concentration of lectins that induces erythrocyte agglutination was measured. The average MAC of intact PNA used in this study was 0.125 μg/mL and 0.79 μg/mL for neuraminidase-treated and neuraminidase-untreated erythrocytes, respectively. The affinity of the intact PNA for Gal-β(1–3)GalNAc was so high that the MAC of the present imaging agent for neuraminidase-treated erythrocytes was lower than that of the old one [24]. The specificity of the imaging agent for Gal-β(1–3)GalNAc detection was extremely superior to that of intact PNA. The other characteristics were similar to those described in our previous article [24].

3.2. In vivo imaging of orthotopic human colorectal tumors in the nude mouse model

Animals with cancer cells invaded to the mucosa of the large intestine are required because the imaging agent has been designed to recognize tumor-derived changes on the mucosal side of epithelial cells. Two types of human colorectal cancer orthotopic animal models have been reported: the implantation of cultured cancer cells in the intestine of immune-deficient animals such as nude and SCID mice [30], and the implantation of fragments of tumor tissues in the intestine [27–29], which was used for our previous study [24]. However, in both cases, since cancer cells and tumor tissues were implanted on the serosal side of the intestine, the animals were required to be maintained until the implanted cancer cells invaded the mucosal side. In the case of the orthotopic HCT-116-RFP nude mouse model where tumor tissues were implanted, we confirmed that a minimum 15-day period was needed for the mucosal invasion of cancer cells from the serosa. Our previous study showed that HT-29-RFP tumor tissues invaded the mucosal side of epithelial cells when mice were maintained for at least 2 weeks after implantation. Differences in cancer cell type did not significantly influence the rate of the mucosal invasion. Nude mice maintained for 21 days after implantation of HCT-116-RFP tumor tissues were used for the studies described below.

Cells contain molecules that fluoresce when excited by UV/Vis light with appropriate wavelength. The endogenous fluorophores-derived fluorescence emission, which is termed autofluorescence, is distinguished from fluorescence signals obtained by exogenous markers. In tissues, extracellular components such as collagen and keratin often contribute to the autofluorescence emission more strongly than do intracellular ones, because they have a relatively high quantum yield [32,33]. Coumarin 6, which is encapsulated into the nanosphere core as an optical component, exhibits a fluorescence emission spectrum at 510–550 nm. It is known that the autofluorescence in the body is seen in spectra similar to those of coumarin 6. Thus, the large intestinal mucosa in HCT-116-RFP tumor tissue-implanted nude mice was observed under fluorescence microscopy in the absence of imaging agents. As shown in Fig. 1, weak autofluorescence was observed on the mucosal surface when an exposure time was set as 1/15 of a second (excitation: 470–495 nm; emission: 510–550 nm); however, the autofluorescence almost disappeared when the exposure time was halved. Phenomena observed in this animal model were similar to those in normal and HT-29-RFP tumor tissue-implanted nude mice in our previous study [24].

In vivo biorecognition of the imaging agent for orthotopic human colorectal tumors was next examined using the HCT-116-RFP tumor tissue-implanted nude mice. The exposure time was set as 1/60 of a second, because we have already confirmed that not only tissue autofluorescence but also nonspecific interactions between normal tissues and the imaging agent are barely observed under these experimental conditions [24]. Fig. 2a shows the fluorescence microphotograph of the large intestinal mucosa treated with the imaging agent at a concentration of 4 mg/mL for 30 min. Imaging agent-derived fluorescence was observed at several sites of the large intestinal mucosa, as seen in the case of HT-29-RFP tumor tissue-implanted nude mice [24]. Clearer specific accumulation of the imaging agent was observed on the large intestinal mucosa treated with the imaging agent at a concentration of 20 mg/mL for 10 min (Fig. 2b). A reduction of the time period required for the biorecognition of the imaging agent for tumors will decrease the time for colonoscopic diagnosis in humans. When HT-29 cells were incubated with the imaging agent in vitro, the fluorescence intensity of the imaging agent-bound cells increased with an increase in the concentration of the agent and with an extension of the incubation time (data not shown). It appears that rapid diagnosis of small-sized colorectal cancers can be realized through an increase in the concentration of the imaging agent.

3.3. In vivo imaging of orthotopic human colorectal tumors in the SCID mouse model

Instead of the orthotopic tumor tissue-implantation model, hereafter, the orthotopic cancer cell-implantation model was used due to its simplicity for developing orthotopic models with mucosal invasion of several types of human colorectal cancer cells. Zamai et al. have succeeded in preparing the orthotopic cancer cell-implantation model by implanting directly with HT-29 cells on the cecal serosa of nude mice. However, since their report had no information on the mucosal invasion of cancer cells from the serosa, we first examined the time period needed for the mucosal invasion. SCID mice, which are deficient in both T and B lymphocytes,

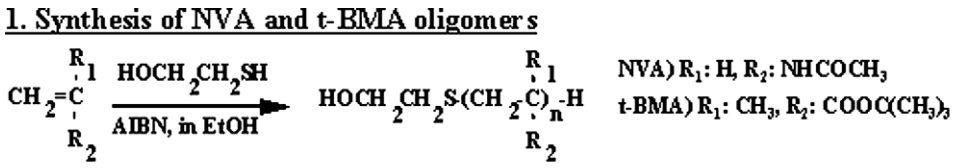

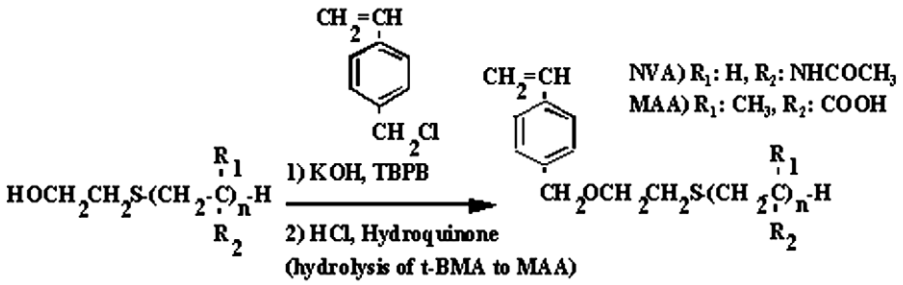

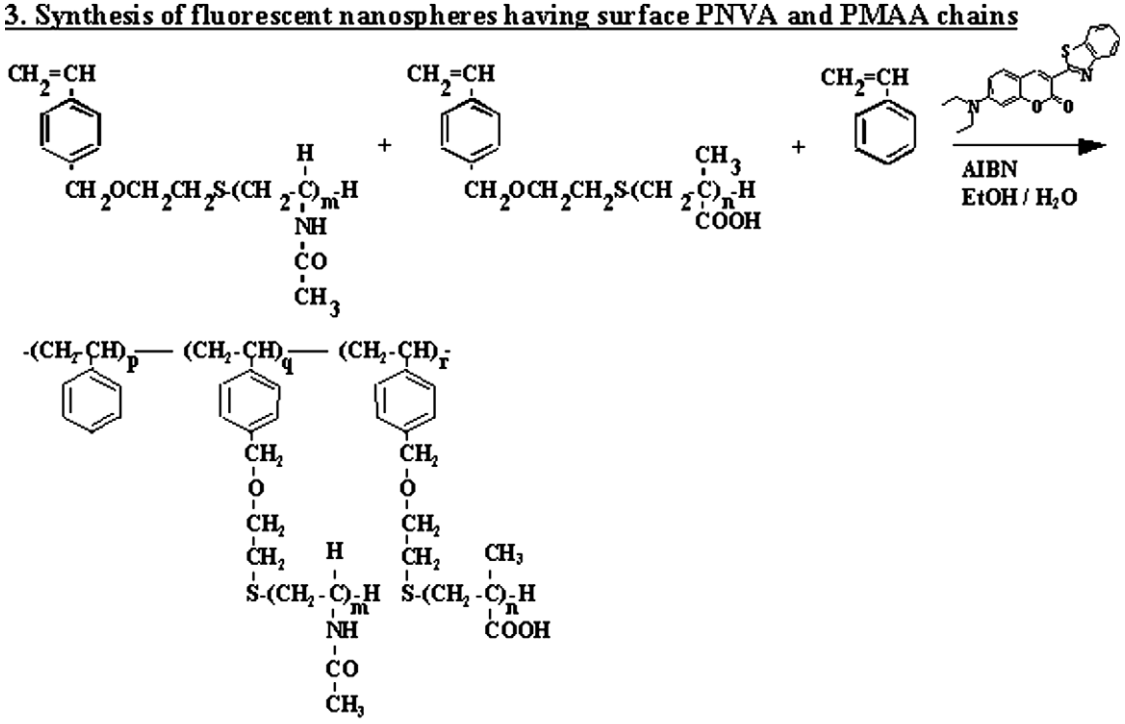

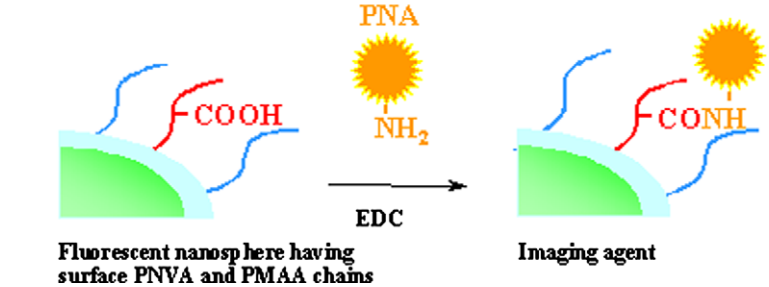

Scheme 1. Synthesis procedures of the imaging agent.

Table 1
Characterization of fluorescent nanospheres having surface PNVA and PMAA chains and PNA-immobilized ones.

Characterization	Fluorescent nanospheres having surface PNVA and PMAA chains	PNA-immobilized fluorescent nanospheres having surface PNVA chains
Average molecular weight of PNVA (Mw/Mn)	9500/4000	←
Average molecular weight of PMAA (Mw/Mn)	10,000/5600	←
Particle size (nm)[a]	181 ± 48	n.t.[h]
Zeta potential (mV)	−23.0	n.t.[h]
NVA/MAA[b]	0.40/0.60	←
Coumarin 6 encapsulated (%, w/w)[c]	0.15[g]	n.t.[h]
Immobilized PNA (μg/mg)[d]	–[i]	3.2
MAC for erythrocytes (μg/mL)[e]	–[i]	>15.0
MAC for neuraminidase-treated ones (ng/mL)[f]	–[i]	0.075

[a] Weight-average diameter (mean ± sd).
[b] Ratio of the number of NVA units to that of MAA units on the nanosphere surface calculated from spectra of electron spectroscopy for chemical analysis.
[c] The weight of coumarin 6 encapsulated in the fluorescent nanospheres per gram of the nanospheres.
[d] Immobilized amount (μg) of PNA per milligram of nanospheres.
[e] Minimum concentration of PNA immobilized on the nanosphere surface that induced erythrocyte agglutination.
[f] Minimum concentration of PNA immobilized on the nanosphere surface that induced neuraminidase-treated erythrocyte agglutination.
[g] Calculated from the residual amount of coumarin 6 in the solvent after copolymerization and the yield of nanospheres.
[h] Not tested.
[i] Not required.

were substituted for nude mice lacking only T lymphocytes. HT-29, HCT-116, or LS174T cells were implanted on the cecal serosa of the mice. Histological evaluation of the cecal mucosa demonstrated that the cancer cells had definitely invaded the mucosal side when the mice were maintained for 6 weeks (HCT-116 and LS174T) and 7 weeks (HT-29) after implantation. When SCID mice, maintained for 4 weeks (HCT-116 and LS174T) and 5 weeks (HT-29) after implantation, were sacrificed for histological evaluation, mucosal invasion was not observed. It was revealed that the mucosal invasion of orthotopically implanted cancer cells was slower than that of orthotopically implanted tumor tissues. SCID mice maintained for 50 days after implantation of the respective cancer cells were used for the studies described below.

Autofluorescence in normal and cancer cell-implanted SCID mice was examined, as carried out for tumor tissue-implanted nude mice (data not shown). Weak autofluorescence was observed on the mucosal surface of the cecum in normal SCID mice when the exposure time of the fluorescence microscope was set as 1/15 of a second; however, it almost disappeared when the exposure time was halved. No significant change in the autofluorescence was observed after orthotopic implantation of any cancer cell type. It was also confirmed that there was no difference in autofluorescence between tumor tissue- and cancer cell-implantation models.

Fig. 3 shows the fluorescence microphotographs of the cecal mucosa in normal and cancer cell-implanted SCID mice treated with the imaging agent at a concentration of 20 mg/mL for 10 min. As shown in Fig. 3b–d, imaging agent-derived fluorescence was observed at several sites of the cecal mucosa in SCID mice implanted orthotopically with cancer cells, irrespective of cancer cell type. The size was of the magnitude of several millimeters. In normal SCID mice, without orthotopic implantation, the fluorescence intensity on the mucosal surface was extremely low and specific accumulation of the imaging agent was not observed (Fig. 3a). This indicated that the nonspecific interactions between normal tissues and the imaging agent were not very strong. These results were similar to those of our previous study using nude mice implanted with HT-29-RFP and HCT-116-RFP tumor tissue fragments. Specific accumulation of the imaging agent on the intestinal mucosa in cancer cell-implanted SCID mice (Figs. 3b–d) and the absence of the specific accumulation in normal mice (Fig. 3a) strongly indicated that PNA-immobilized fluorescent nanospheres recognized tumor-derived changes on the mucosal surface (i.e., the expression of the TF antigen) through PNA-binding to Gal-β(1–3)GalNAc residues. It was probable that there was biorecognition of the imaging agent for the mucosal invasion of human colorectal cancer cells independent of cell type.

To confirm that the imaging agent interacted only with cancer cells exposed on the cecal mucosa, microscopic histological evaluation was carried out using tissue pieces excised from the cecum of HT-29 and HCT-116 cell-implanted SCID mice treated with the imaging agent at a concentration of 20 mg/mL for 10 min. As shown in Table 2, cancer cells were present in the mucosal epithelia when the imaging agent gave rise to fluorescence, irrespective of the implanted cancer cell type. In contrast, cancer cells were absent from the mucosal epithelia without the fluorescence, except in one case of HCT-116 cell-implanted SCID mice. A good correlation was generally observed; however, the exception suggests a difference in the time period that is required for biorecognition between HT-29 and HCT-116 cells.

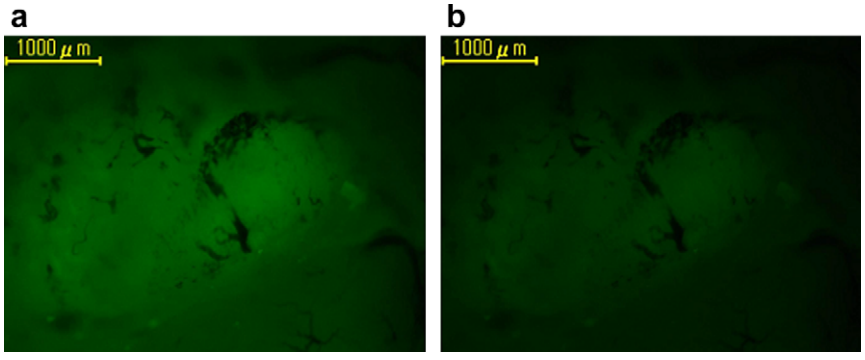

Fig. 1. Fluorescence microphotographs of the large intestinal mucosa in HCT-116-RFP tumor tissues-implanted nude mice. Pictures were obtained using the fluorescence microscope (magnification: 40×; excitation: 470–495 nm; emission: 510–550 nm). Autofluorescence of the mucosa was observed at an exposure time of 1/15 of a second (a) and 1/30 of a second (b).

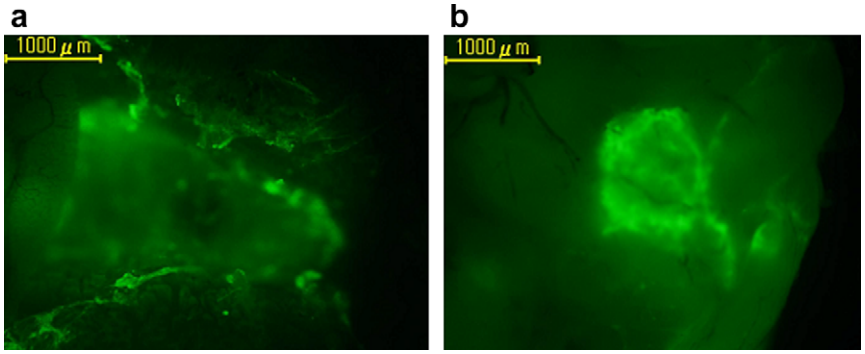

Fig. 2. Fluorescence microphotographs of the large intestinal mucosa in orthotopic HCT-116-RFP tumor tissue-implanted nude mice. Mice were sacrificed on the 21st day after surgical orthotopic implantation. A 3-cm loop of the tumor-bearing ascending colon was then prepared. The luminal side of the colon was treated with the imaging agent, washed with calcium ion-containing PBS, and then observed under fluorescence microscopy (magnification: 40×; excitation: 470–495 nm; emission: 510–550 nm; exposure: 1/60 of a second). Images a and b correspond to fluorescence microphotographs of the large intestinal mucosa treated with the imaging agent at a concentration of 4 mg/mL for 30 min and 20 mg/mL for 10 min, respectively.

We have investigated in vitro interactions among the imaging agent and various types of human colorectal cancer cells [24]. Cultured cancer cells were incubated with the imaging agent at a concentration of 2 mg/mL for 30 min, cells were separated from unbound imaging agent, and then the fluorescence intensity of imaging agent-bound cells was estimated quantitatively, using image analysis. The fluorescence intensity of the cancer cells was higher than that of the human small intestinal epithelial cells, which were used as a negative control. The difference between cancer cells and normal cells with regard to biorecognition probably resulted from the presence or absence of surface Gal-β(1–3)GalNAc residues. In vitro cell studies demonstrated that the imaging agent bound to colorectal cancer cells with high affinity and specificity. However, there were also differences in the intensity of fluorescence among the cancer cells. The order of the fluorescence intensity, which possibly corresponds to the expression level of the TF antigen, was HT-29 > HCT-116 > LS174T. The time period required for biorecognition of the imaging agent against HCT-116 cell-derived tumors may be longer than that for HT-29 cell-derived tumors.

To verify this speculation, the same test was repeated for cancer cell-implanted SCID mice, with changes made to incubation time. The incubation time of the imaging agent with the cecal mucosa in HCT-116 cell-implanted SCID mice was extended to 30 min, but that in HT-29 cell-implanted SCID mice was reduced to 1 min. Similar accumulation of the imaging agent on the cecal mucosa in the orthotopic animal model was observed, irrespective of incubation time (data not shown). Table 3 shows the results of

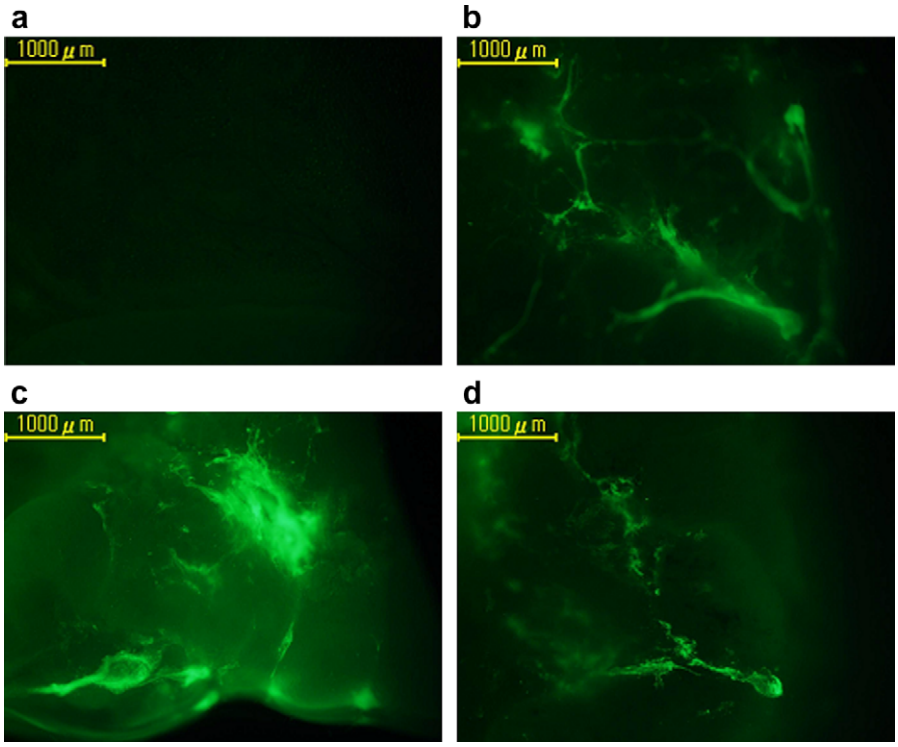

Fig. 3. Fluorescence microphotographs of the cecal mucosa in normal (a), HT-29 cell- (b), HCT-116 cell- (c), and LS174T cell-implanted (d) SCID mice treated with the imaging agent at a concentration of 20 mg/mL for 10 min. Mice were sacrificed on the 50th day after orthotopic implantation. A 3-cm loop of the tumor-bearing cecum was then prepared. The luminal side of the cecum was treated with the imaging agent, washed with calcium ion-containing PBS, and then observed under fluorescence microscopy (magnification: 40×; excitation: 470–495 nm; emission: 510–550 nm; exposure: 1/60 of a second).

Table 2
Histological evaluation of tissue pieces excised from the cecum of cancer cell-implanted SCID mice treated with the imaging agent for 10 min.

Model: HT-29 cell-implanted SCID mice; Incubation time: 10 min												
Samples	bright piece 1			bright piece 2			dark piece 1			dark piece 2		
slice positions (μm)	600	1500	2400	600	1500	2400	400	1000	1600	600	1500	2400
lamina muscularis mucosae	-*	-*	-*	+*	+*	+*	-*	-*	-*	-	-	-*
lamina propria mucosae	+*	+*	+*	+*	+*	+*	+*	-*	-*	-	-	-*
mucosal epithelia	+	+	+	-	+	+	-	-	-	-	-	-
+: invasion of implanted cancer cells; -: no invasion; * the invasion was observed in blood and/or lymph vessels												
Model: HCT-116 cell-implanted SCID mice; Incubation time: 10 min												
Samples	bright piece 1			bright piece 2			dark piece 1			dark piece 2		
slice positions (μm)	600	1500	2400	600	1500	2400	600	1500	2400	600	1500	2400
lamina muscularis mucosae	+*	+*	-	-*	+*	-*	+*	+*	+*	+*	+*	+*
lamina propria mucosae	+*	+*	+	+*	+*	-	-	-	-	+*	+*	+*
mucosal epithelia	+	+	+	+	+	-	-	-	-	+	+	-
+: invasion of implanted cancer cells; -: no invasion; * the invasion was observed in blood and/or lymph vessels												

Table 3
Histological evaluation of tissue pieces excised from the cecum of cancer cell-implanted SCID mice treated with the imaging agent for 1 or 30 min.

Model: HT-29 cell-implanted SCID mice; Incubation time: 1 min												
Samples	bright piece 1			bright piece 2			dark piece 1			dark piece 2		
slice positions (μm)	900	1800	2700	400	1000	1600	600	1500	2400	400	1000	1600
lamina muscularis mucosae	+*	+*	+*	-*	-*	-*	-	-*	-	-*	-*	-
lamina propria mucosae	+*	+*	+*	+*	+*	+*	-	-	-	+*	-*	-
mucosal epithelia	+	+	-	+	+	+	-	-	-	-	-	-
+: invasion of implanted cancer cells; -: no invasion; * the invasion was observed in blood and/or lymph vessels												
Model: HCT-116 cell-implanted SCID mice; Incubation time: 30 min												
Samples	bright piece 1			dark piece 2			dark piece 1			dark piece 2		
slice positions (μm)	600	1500	2400	600	1500	2400	400	1000	1600	400	1000	1600
lamina muscularis mucosae	+	+*	+*	+*	+*	+*	-*	+*	+*	-*	-*	-*
lamina propria mucosae	+	+	+	+	+	+	-	+	+	-	-	-
mucosal epithelia	+	+	+	+	+	+	-	-	-	-	-	-
+: invasion of implanted cancer cells; -: no invasion; * the invasion was observed in blood and/or lymph vessels												

microscopic histological evaluation. Bright and dark pieces completely denoted the presence and absence, respectively, of the invasion of implanted cancer cells on mucosal epithelia. A comparison of Table 3 with Table 2 indicates that tumors exposed on the mucosal side of the epithelial cells will be detected by the imaging agent if they are in contact with each other for the time period that is sufficient for PNA-induced biorecognition. The time period possibly depends on the cancer cell type, and the dependence may be due to the different expression levels of the TF antigen in each cell type.

3.4. Behavior of the imaging agent in large intestinal mucosa with bowel diseases other than cancer

Patients with colorectal cancer often suffer from complications arising from other bowel diseases. As described in the previous section, we clearly demonstrated that the imaging agent recognized millimeter-sized tumors in the large intestinal mucosa with high affinity and specificity, but the imaging agent should also distinguish colorectal cancer from these bowel diseases. Inflammatory bowel diseases such as ulcerative colitis are common, and we therefore examined the interactions between the imaging agent and ulcers in the large intestinal mucosa using a conventional animal model with DSS-induced ulcerative colitis.

There was no detectable autofluorescence when the large intestinal mucosa in SCID mice with DSS-induced ulcerative colitis was observed under fluorescence microscopy at an exposure time of 1/30 of a second (Fig. 4). This indicated that colitis induction by DSS did not influence autofluorescence. The large intestinal mucosa with ulcers was next treated with the imaging agent. As shown in Fig. 5a and b, the fluorescence intensity was extremely low when the mucosal surface was observed under fluorescence microscopy at an exposure time of 1/60 of a second, during which

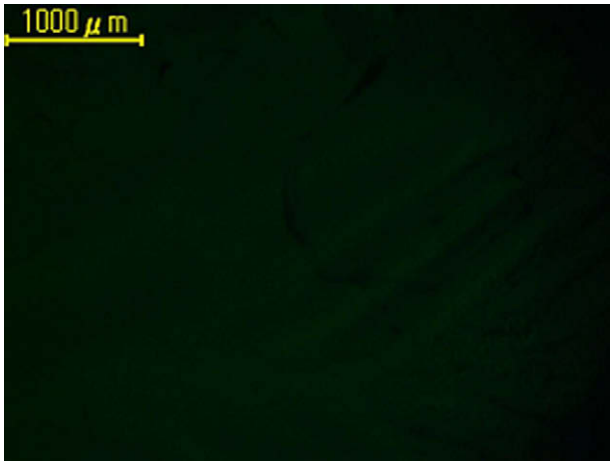

Fig. 4. Fluorescence microphotograph of the large intestinal mucosa in SCID mice with ulcerative colitis. The picture was obtained using the fluorescence microscope (magnification: 40×; excitation: 470–495 nm; emission: 510–550 nm; exposure: 1/30 of a second).

nonspecific interactions between normal tissues and the imaging agent were barely observed. Since the nonspecific interactions between ulcerative tissues and the imaging agent were not very strong, we concluded that the imaging agent could distinguish colorectal cancer from ulcerative colitis. However, as shown in Fig. 5c and d obtained at an exposure time of 1/30 of a second, the fluorescence intensity tended to increase with an increase in incubation time. The TF antigen has also been identified in precancerous conditions such as inflammatory bowel diseases, although the expression level in ulcerative colitis was lower than that in colonic adenocarcinoma in humans [17,20]. Small amounts of the imaging agent possibly bound to ulcers through PNA-induced rec-

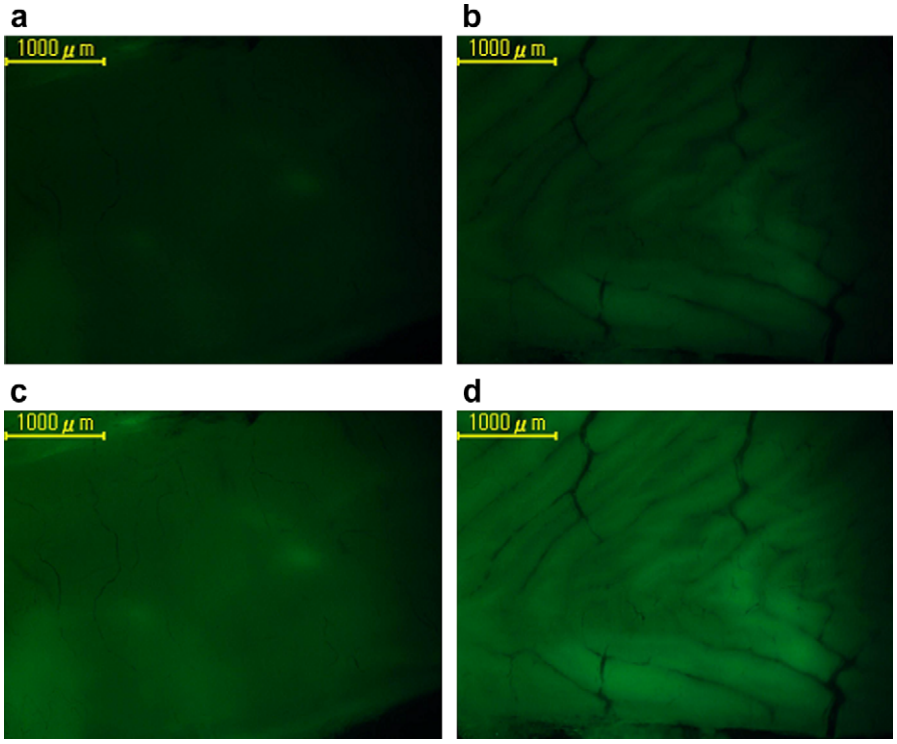

Fig. 5. Fluorescence microphotographs of the large intestinal mucosa in SCID mice with ulcerative colitis treated with the imaging agent at a concentration of 20 mg/mL for 10 min (a and c) and 30 min (b and d). After oral administration of DSS aqueous solution for 9 days, mice were sacrificed, and a 3-cm loop of the descending colon with ulcers was then prepared. The luminal side of the colon was treated with the imaging agent, washed with calcium ion-containing PBS, and then observed under fluorescence microscopy (magnification: 40×; excitation: 470–495 nm; emission: 510–550 nm). Images were obtained at an exposure time of 1/60 of a second (a and b) and 1/30 of a second (c and d).

ognition when the mucosal surface was exposed to the agent for an extended period, although the difference in binding to cancerous and inflamed tissues should be minutely characterized because colorectal cancer is often complicated by inflammatory bowel diseases.

The latest data described in this report encourage us to evaluate the clinical potential of the imaging agent in the future; however, there are several issues that must be settled for the clinical trial. It is important to estimate the lower limit of tumor detection with the imaging agent. A quantitative discussion based on an assay of Gal-β(1–3)GalNAc residues will be needed. The behavior of fluorescent nanospheres decorated with other lectins such as wheat germ agglutinin that binds to healthy tissues on the large intestinal mucosa should be compared with that of the imaging agent. We have just started to evaluate the safety of the imaging agent. The productivity, specifications, and the chemical stability of the imaging agent should be also examined. These studies will be carried out successively.

4. Conclusions

PNA-immobilized fluorescent nanospheres with surface PNVA chains encapsulating coumarin 6 were designed as an endoscopic imaging agent for the detection of early colorectal cancer. The in vivo performance of the imaging agent was ascertained using SCID and nude mice that had been orthotopically implanted with several types of human colorectal adenocarcinoma cell lines. Imaging agent-derived fluorescence was observed at several sites of the cecal mucosa after the luminal side of the tumor-bearing cecum was treated with the agent, irrespective of cancer cell type. Microscopic histological evaluation revealed that the imaging agent bound to cancer cells on the mucosal surface with high affinity and specificity. It appeared that the imaging agent could distinguish neoplastic mucosal changes from those induced by other bowel diseases. We concluded that PNA-immobilized fluorescent nanospheres are a potential candidate for use as a colonoscopic imaging agent.

Acknowledgments

This work was financially supported in part by a Grant-in-aid for a research for promoting technological seeds from Japan Science and Technology Agency (JST) and a grant-in-aid from the Sagawa foundation for promotion of cancer research. The authors thank Showa Denko Co. and Applied Medical Research Laboratory Inc. (Osaka, Japan) for the gift of NVA monomers and for the histological evaluation of tumor tissues, respectively.

References

[1] A. Jemal, R. Siegel, E. Ward, T. Murray, J. Xu, C. Smigal, M.J. Thun, Cancer statistics, CA Cancer J. Clin. 56 (2) (2006) 106–130.
[2] <http://www.cancer.gov>.
[3] G.C. Balch, A. De Meo, J.G. Guillem, Modern management of rectal cancer: a 2006 update, World J. Gastroenterol. 12 (20) (2006) 3186–3195.
[4] T. Muto, M. Oya, Recent advances in diagnosis and treatment of colorectal T1 carcinoma, Dis. Colon Rectum 46 (Suppl.. 10) (2003) S89–S93.
[5] T. Ponchon, Endoscopic mucosal resection, J. Clin. Gastroenterol. 32 (1) (2001) 6–10.
[6] S. Kudo, Y. Tamegai, H. Yamano, Y. Imai, E. Kogure, H. Kashida, Endoscopic mucosal resection of the colon: the Japanese technique, Gastrointest. Endosc. Clin. North Am. 11 (3) (2001) 519–535.
[7] B. Rembacken, T. Fujii, H. Kondo, The recognition and endoscopic treatment of early gastric and colonic cancer, Best Prac. Res. Clin. Gastroenterol. 15 (2) (2001) 317–336.
[8] H. Kashida, S. Kudo, Early colorectal cancer: concept, diagnosis, and management, Int. J. Clin. Onco. 11 (1) (2006) 1–8.
[9] J.J. Tischendorf, H.E. Wasmuth, A. Koch, H. Hecker, C. Trautwein, R. Winograd, Value of magnifying chromoendoscopy and narrow band imaging (NBI) in

classifying colorectal polyps: a prospective controlled study, Endoscopy 39 (12) (2007) 1092–1096.
[10] R.S. DaCosta, B.C. Wilson, N.E. Marcon, Fluorescence and spectral imaging, Scientific World J. 7 (2007) 2046–2071.
[11] K. Kelly, H. Alencar, M. Funovics, U. Mahmood, R. Weissleder, Detection of invasive colon cancer using a novel, targeted, library-derived fluorescent peptide, Cancer Res. 64 (17) (2004) 6247–6251.
[12] S. Anandasabapathy, Endoscopic imaging: emerging optical techniques for the detection of colorectal neoplasia, Curr. Opin. Gastroenterol. 24 (1) (2008) 64–69.
[13] F.J. van der Broek, P. Fockens, E. Dekker, New development in colonic imaging, Aliment Pharmacol. Ther. (Suppl. 2) (2007) 91–99.
[14] M. Hirata, S. Tanaka, S. Oka, I. Kaneko, S. Yoshida, M. Yoshihara, K. Chayama, Evaluation of microvessels in colorectal tumors by narrow band imaging magnification, Gastrointest. Endosc. 66 (5) (2007) 945–952.
[15] K. Hiwatari, S. Sakuma, K. Iwata, Y. Masaoka, M. Kataoka, H. Tachikawa, Y. Shoji, S. Yamashita, Poly(*N*-vinylacetamide) chains enhance lectin-induced biorecognition through the reduction of nonspecific interactions with non-targets, Eur. J. Pharm. Biopharm. 70 (2) (2008) 453–461.
[16] C.R. Boland, J.A. Roberts, Quantitation of lectin binding sites in human colon mucins by use of peanut and wheat germ agglutinin, J. Histochem. Cytochem. 36 (10) (1988) 1305–1307.
[17] B.J. Campbell, I.A. Finnie, E.F. Hounsell, J.M. Rhodes, Direct demonstration of increased expression of Thomsen-Friedenreich (TF) antigen from colonic adenocarcinoma and ulcerative colitis mucin and its concealment in normal mucin, J. Clin. Invest. 95 (2) (1995) 571–576.
[18] J. Samuel, A. Noujaim, G. MacLean, M. Suresh, B. Longenecker, Analysis of human tumor associated Thomsen-Friedenreich antigen, Cancer Res. 50 (15) (1990) 4801–4808.
[19] F. Schneider, W. Kemmner, W. Haensch, G. Franke, S. Gretschel, U. Karsten, P. Schlag, Overexpression of sialyltransferase CMP-sialic acid: Galβ1,3GalNAc-R α6-sialyltransferase is related to poor patient survival in human colorectal carcinoma, Cancer Res. 61 (11) (2001) 4605–4611.
[20] S. Wróblewski, M. Berenson, P. Kopečková, J. Kopeček, Potential of lectin-N-(2-hydroxypropyl)methacrylamide copolymer-drug conjugates for the treatment of pre-cancerous conditions, J. Control. Release 74 (1–3) (2001) 283–293.
[21] S. Sakuma, Z.-R. Lu, P. Kopečková, J. Kopeček, Biorecognizable HPMA copolymer-drug conjugates for colon-specific delivery of 9-aminocamptothecin, J. Control. Release 75 (3) (2001) 365–379.
[22] S. Sakuma, R. Sudo, N. Suzuki, H. Kikuchi, M. Akashi, M. Hayashi, Mucoadhesion of polystyrene nanoparticles having surface hydrophilic polymeric chains in the gastrointestinal tract, Int. J. Pharm. 177 (2) (1999) 161–172.
[23] S. Sakuma, M. Hayashi, M. Akashi, Design of nanoparticles composed of graft copolymers for oral peptide delivery, Adv. Drug Deliv. Rev. 47 (1) (2001) 21–37.
[24] S. Sakuma, T. Yano, Y. Masaoka, M. Kataoka, K. Hiwatari, H. Tachikawa, Y. Shoji, R. Kimura, H. Ma, Z. Yang, L. Tang, R.M. Hoffman, S. Yamashita, In vitro/in vivo biorecognition of lectin-immobilized fluorescent nanospheres for human colorectal cancer cells, J. Control. Release 134 (1) (2009) 2–10.
[25] M. Akashi, T. Niikawa, T. Serizawa, T. Hayakawa, M. Baba, Capture of HIV-1 gp120 and virions by lectin-immobilized polystyrene nanospheres, Bioconjug. Chem. 9 (1) (1998) 50–53.
[26] S. Sakuma, N. Suzuki, R. Sudo, K. Hiwatari, A. Kishida, M. Akashi, Optimized chemical structure of nanoparticles as carriers for oral delivery of salmon calcitonin, Int. J. Pharm. 239 (1–2) (2002) 185–195.
[27] <http://www.anticancer.com/>.
[28] S. Togo, H. Shimada, T. Kubota, A. Moossa, R.M. Hoffman, Host organ specifically determines cancer progression, Cancer Res. 55 (3) (1995) 681–684.
[29] M. Yang, L. Li, P. Jiang, A.R. Moossa, S. Penman, R.M. Hoffman, Dual-color fluorescence imaging distinguishes tumor cells from induced host angiogenic vessels and stromal cells, Proc. Natl. Acad. Sci. USA 100 (24) (2003) 14259–14262.
[30] M. Zamai, M. vandeVen, M. Farao, E. Gratton, A. Ghiglieri, M. Castelli, E. Fontana, R. d'Argy, A. Fiorino, E. Pesenti, A. Suarato, V. Caiolfa, Camptothecin poly[N-(2-hydroxypropyl)methacrylamide] copolymers in antitopoisomerase-I tumor therapy: intratumor release and antitumor efficacy, Mol. Cancer Ther. 2 (1) (2003) 29–40.
[31] I. Murakami, Y. Hamada, S. Yamane, H. Fujino, S. Horie, T. Murayama, Nicotine-induced neurogenic relaxation in the mouse colon: changes with dextran sodium sulfate-induced colitis, J. Pharmacol. Sci. 109 (1) (2009) 128–138.
[32] W. Zheng, Y. Wu, D. Li, J.Y. Qu, Autofluorescence of epithelial tissue: single-photon versus two-photon excitation, J. Biomed. Opt. 13 (5) (2008) 054010.
[33] M. Monici, Cell and tissue autofluorescence research and diagnostic applications, Biotechnol. Annu. Rev. 11 (2005) 227–256.